The composite shear and tension failure through the intact rock in these tests is an interesting one. In Sample No. 28, branch cracks developed from the joint ends. The tension fractures took place along these surfaces and the shear failures took place on distinctly different planes, almost at right angles to these tension surfaces. This is probably the closest that one gets to the idealized step joint failure mechanism, as depicted in Figure 1.2.5.1(b) in these tests. Far more common, in these tests, was the step failure on a smaller scale. Lots of separate, small striations, in the α-direction, were observed on many of the failure surfaces. These could easily be seen when looking at the failure surface in a direction at right angles to the plane of the sample, i.e. in the same direction in which the photographs were taken. If the failure surface was observed at right angles to this direction, in the α-direction, a projection of the failure surface was seen that looked very like the tension failure surfaces observed on the dog-bone tension test pieces. This suggested to the author that a step failure had occurred on a small scale, with small, yet distinct, tension and shear failures occurring. The failure surface would thus tend to oscillate about a mean plane as it stepped. This did tend to show up, with the mean plane very often being, not unexpectedly, the plane between the two joint ends (e.g. Sample Nos. 15 and 29).

The failure loads of these samples were not consistent and seem hardly worth averaging. However, they do tend to

i/ increase as α increases, and

ii/ increase as L increases

as would be expected.

2.5.3 Class 3 Results

Class 3 failures proved to be very straightforward. Shear, or slip, took place along the α-joint planes (in the α-direction), separation took place along the ψ-joint and a tension fracture took place through the intact material from the end of the ψ-joint to the α-joint (approximately) perpendicular to the α-joint. It will be noticed that all but one of the mechanisms envisaged by Jennings (that of shear through the intact material) occurred in both of these tests. The make up of a Class 3 configuration leaves little opportunity for this mode to occur. Class 3 configurations are, therefore, a special case of Class 2 configurations in that the ψ-joint defines the position at which stepping down from one α-joint to another occurs.

Because the mode of failure of these samples was so straightforward, only two Class 3 samples were tested. These are Sample No. 8 and the sample whose photograph precedes [illegible]. Both photographs show all three modes of failure.

2.5.4 Class 4 Results

Of the four classes tested, Class 4 probably yielded the least satisfactory results. Three times the joint pieces slipped from their intended positions before the plaster of paris hardened (Sample Nos. 51, 57 and 59). Twice the actual joint pieces interfered with the failure through the intact material (Sample Nos. 56 and 57). In addition, Sample No. 5 had a strange and unforseen mode of failure and should, possibly, be disregarded. However, in this case, it should be pointed out that, because of the low value of α and the high values of s and t, the "weakening effect" of the joints was low and the higher stresses necessitated by this low "weakening effect" always increase the likelihood of material failure (e.g. spalling), as opposed to failure governed entirely by the joint configuration, occurring. All the tests have, nevertheless, been documented.

In these Class 4 tests, the "expected" mode of failure was a two-dimensional movement in the α-direction with joint shear, separation along the ψ-joint and shear through the intact material occurring; with tension through intact material between the joints taking place if required by the specific joint configuration. With notable exceptions, e.g. Nos. 5 and 56 (which could easily be discarded), this was roughly the mode that was observed.

For negative values of t, where no tension fracture through the intact material was necessary, two of the samples (Nos. 50 and 52) showed the expected mechanisms of joint shear, separation along the ψ-joint and shear along the extension of the α-joint very nicely. The other two samples showed separation along only part of the ψ-joint. This necessitated a tensile as well as a shear component of failure through the intact material between the joints (Sample Nos. 53 and 55). For $t = 0$, separation

has again not taken place along the whole ψ-joint. This has again required a tensile as well as a shear component of failure through the intact material between the joints (Sample No. 54).
Where t has been positive, failure has largely (with the exception of Sample No. 5) occurred as expected with the mechanisms being shear along the α-joints, separation along the ψ-joint and a combined shear and tension failure through the intact material between the joints. The photograph of Sample No. 7 shows a nice example. Separation has not always occurred along the whole of the length of the ψ-joint. This has meant more tensile fracture through the intact material than was necessary, e.g. sample Nos. 7, 58 and 60.

To summarize then: the modes of failure of the Class 4 samples depended largely on the value of t (whether it was positive, zero or negative). In all cases slippage was observed along the α-joints. In most cases separation occurred along the ψ-joint. For negative values of t, either a fairly planar shear failure along the extension of the α-joint or a combined shear and tension failure (which shortened the separation along the ψ-joint) occurred through the intact material (Sample Nos. 52 and 53). For values of t equal to zero, separation did not take place over the whole length of the ψ-joint and this separation was joined to the shear failure along the α-joint by a combined shear and tension failure through the originally intact material (Sample No. 54). For positive values of t, separation took place along all, or most, of the ψ-joint length and this separation failure was joined to the shear failure along the lower α-joint by a combined shear and tension failure through the intact material (Sample Nos. 58 and 61).

TABLE 2.3 FAILURE DETAILS OF THE CLASS 4 SAMPLES TESTED

SAMPLE NO.	α (°)	S (mm)	t (mm)	W (kN)	FAILURE MECHANISMS OBSERVED					
					JS	SJ	S1	T1	BC	S
3	30	115	63	64,5	2	2	2	2		
5	30	116	65	64,0	2		2	?	?	2
7	40	60	21	9,5	2	2	2	2		
50	40	38	-25	13,2	2	2	2			
52	39½	33	-25	?	2	2	2			
53	39½	35	-25	20,0	2	2	2	2		
54	39	32	0	9,9	2	2	2	2		
55	38½	40	-25	21,1	2	2	2	2		
56	39	32	0	9,9	2		1	2	?	
58	39	59	25	12,7	2	2	2	2		
60	40	59	25	18,1	2	2	2	2	1	1
61	39½	59	25	22,7	2	2	2	2		

JS stands for shear along joint surfaces

SJ stands for separation along ψ-joint surfaces

S1 stands for shear through intact material

T1 stands for tension fracture linking two joints through originally intact material

BC stands for branch cracks

S stands for spalling of material off the sides of the block

2 indicates a major participation in the failure

1 indicates a minor influence on the failure

2.5.5 Summary of Results

In conclusion, four things may be said about the results in general. These are:

1/ The mechanisms observed seem to be typical of those involved in brittle fracture.

2/ The discontinuities affected the failure of all of the samples.

3/ It can by no means be said that the failure of all the samples was entirely two-dimensional. However, enough tests were carried out for the three-dimensional effects to be observed, isolated and disregarded.

4/ Different failure mechanisms were observed and recognized.

A discussion on these individual failure mechanisms recognized in the tests will now follow.

1/ Shear movement along joint surfaces

This failure mode occurred in all joint configuration classes. It always had to occur with at least one other mode. The mechanism here is the relative movement of the two flat plaster of paris surfaces forming a joint (in the direction of the joint).

See photographs of Sample Nos.: 1 (Class 1)
2 (Class 2)
8 (Class 3)
7 (Class 4)

2/ Separation along a joint

This mode occurred only in Classes 3 and 4 where the relative movement of the two parts of the block occurred in the α-direction. The ψ-joint provided a convenient plane of weakness along which separation could take place in an effort to join the two separate shear failures. Separation thus took place along the ψ-joint, partially linking the two shear failures on the α-joints; see photographs of Sample Nos.: 8 (Class 3)

50 (Class 4).

3/ Clean Tension Fracture

This mode of failure consists of a clean tension fracture of the originally intact material between two joints. In Class 3 configurations it joins the shear failure along an α-joint to the separation along a ψ-joint (see Sample No. 8). In Class 2 configurations it links the two shear failure surfaces along the α-joints. It does not occur in Class 1 nor in Class 4 configurations.

With the relative movement of the two parts of the block occurring in the α-direction, one might expect the tension fractures to take place perpendicular to the α-joints. While this is approximately true in most cases, it is seldom, if ever, exactly true. See photographs of Sample Nos.: 8 (Class 3)

2 (Class 2).

4/ Branch Cracks

These cracks started at or near the ends of joints and grew, gradually migrating into the direction of compression. They were often noticed before peak load had been reached. The cracks occurred in joint configuration Classes 1, 2 and 4 and sometimes developed into near vertical tension fractures.
See photographs of: Sample No. 1 (Class 1)

Branch crack starting near joint end

Sample No. 18 (Class 2)

Sample No. 51 (Class 4).

5/ Tension Fracture (or axial cleavage) resulting from branch cracks

This failure mode consists of near vertical tension fractures through the originall intact material which normally start at or near joint ends and very often take the shape of branch cracks. The mode occurs in Class 1 and Class 2 configurations. See photographs of Sample Nos.: 1 (Class 1)

6 (Class 1)

11 (Class 2)

PHOTOGRAPH OF A BRANCH CRACK STARTING NEAR A JOINT END. STRIATIONS IN THE α-DIRECTION CAN ALSO BE SEEN

6/ Plane Shear

This mode consists of a fairly planar shear failure through originally intact material along the extension of an α-joint. It occurred in Classes 1 and 4 where it connected a shear failure along an α-joint to either another such failure or to a separation failure along a ψ-joint, respectively. See photographs of Sample Nos.: 6 (Class 1)

50 (Class 4)

70 (Class 1)

7/ Combined shear and tension fracture through intact material

These are failures leaving failure surfaces which show evidence of both tension fracture and shear movement through the intact material either on a micro- or a macro- scale. Evidence of tension fracture is seen by looking, in the α-direction, at a failure surface and observing the projection which

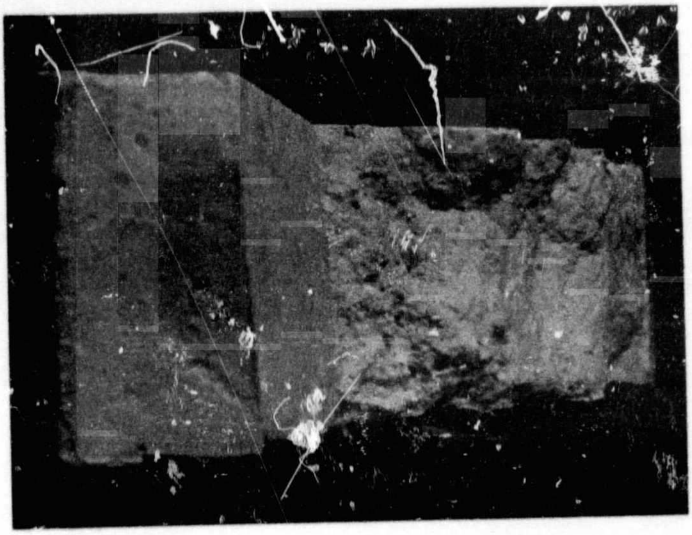

PHOTOGRAPH OF THE PROJECTION OF A FAILURE SURFACE SHOWING TENSION FRACTURE

looks like the failure surfaces of the dog-bone samples. Evidence of shear movement through the intact material is given by the striations in the α-direction observed on the failure surfaces. These separate failures, of whatever size, occurring next to one another, give the failure surface its final shape. This mode occurs in Classes 2 and 4. See photographs of Sample Nos.: 11 (Class 2)

15 (Class 2)

28 (Class 2)

29 (Class 2)

7 (Class 4)

8/ Spalling

This mode is a lot like the spalling of concrete off a reinforced concrete column. It tends to occur between the joints, where the plaster of paris is acting as a column. Pieces spall off one or both sides of the sample and the failure surfaces are not unlike those obtained when the cylindrical samples of plaster were tested in unconfined compression. Spalling occurred in Classes 1, 2 and 4, but there is no reason for it not to occur in Class 3 configurations if higher stresses are encountered. It is a three-dimensional effect.

See photographs of Sample Nos.: 1 (Class 1)

6 (Class 1)

20 (Class 2)

Failure modes 1, 2, 3, 6 and 7 tended to occur when the weakening effect of the joints was great (i.e large α and large continuity). Failure modes 4, 5 and 8), however, tended to occur when the weakening effect of the joints was not very great (i.e. small α and small continuity).

CHAPTER 3

SOME CALCULATIONS AND CONCLUSIONS

Chapter 3

Introduction

In this chapter a comparison is made between the strength values obtained in the tests described and calculated strength values. The calculations have been made according to the equations of Jennings as modified in Chapter 1.

In this chapter the following notation has been used:

W = failure load

A = cross sectional area of sample (= 9" x 2")

C_j and ϕ_j are the shear parameters of the joints

C_m and ϕ_m are the shear parameters of the intact material

A_j = area of joint (= 2" x length of joint)

A_m = area of intact material between joints (Class 1)

T = the thickness of the samples (2")

3.1 Class 1 Calculations

The failure mode assumed for these calculations is two-dimensional shear failure in the α-direction along the plane containing the introduced "joints".

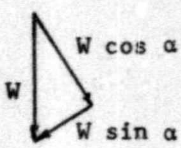

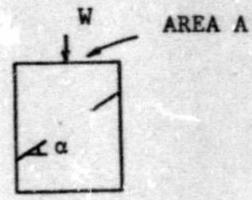

Normal stress on α-plane = $\dfrac{W\cos\alpha}{A/\cos\alpha} = W\cos^2\alpha/A = \sigma_n$.

At failure: DF = RF

$$W\sin\alpha = (C_j + \sigma_n \tan\phi_j)\,A_j + A_m\,(C_m + \sigma_n\tan\phi_m)$$

$$= C_j.A_j + \frac{W}{A}.\cos^2\alpha.\tan\phi_j.A_j + A_m.C_m + A_m.\frac{W}{A}.\cos^2\alpha.\tan\phi_m$$

$$W(\sin\alpha - \frac{A_j}{A}.\cos^2\alpha.\tan\phi_j - \frac{A_m}{A}.\cos^2\alpha.\tan\phi_m) = C_j.A_j + A_m.C_m$$

i.e. $$W = \frac{C_j.A_j + A_m.C_m}{(\sin\alpha - \frac{A_j}{A}.\cos^2\alpha.\tan\phi_j - \frac{A_m}{A}.\cos^2\alpha.\tan\phi_m)}$$

For plaster of paris (C_j = 0,0088 MPa, $\phi_j = 26^o$, C_m = 1,4 MPa and $\phi_m = 41^o$) and 2" thick samples (i.e. A_j = 51 $(L_2 + L_4)$ mm^2, $A_m = 51(L_1 + L_3 + L_5)$ mm^2 ,

$\dfrac{A_j}{A} = \dfrac{L_2 + L_4}{9 \times 25,4}$ and $\dfrac{A_m}{A} = \dfrac{L_1 + L_3 + L_5}{9 \times 25,4}$), we have

$$W = \frac{0,0088.51(L_2 + L_4) + 1,4\,(L_1 + L_3 + L_5).51}{\sin\alpha - \frac{L_2 + L_4}{228,6}.\cos^2\alpha.\tan 26^o - \frac{L_1 + L_3 + L_5}{228,6}.\cos^2\alpha.\tan 41^o}$$

$$= \frac{51\ (0{,}0088\ (L_2 + L_4\ ) + 1{,}4\ (L_1 + L_3 + L_5))}{\sin\alpha - 0{,}00213\ (L_2 + L_4)\cos^2\alpha - 0{,}0038\ (L_1 + L_3 + L_5)\cos^2\alpha}\ \text{N}$$

It can be seen, from the expression for W, that as α decreases, the denominator also decreases and will reach zero at some value of α (depending on the values of L_1, L_2, L_3, L_4 and L_5). (An expression could be found for this value, in terms of L_1, L_2, L_3, L_4 and L_5, by putting the denominator = 0 and solving for α). If the denominator is equal to zero, the sample has, in this mode, an infinitely high strength. If the continuity was equal to one (k = 1), this would occur at $\alpha = \phi_j$ ($\approx 26^o$); the explanation being that the obliquity of the disturbing force on the α-plane would not be great enough to cause failure along it. However, in the tests, the continuity was always less than one so that this stage was always reached in the range $\phi_j < \alpha < \phi_m$ ($26^o < \alpha < 41^o$), depending on the values of L_1, L_2, L_3, L_4 and L_5. If α were decreased further a negative denominator would be obtained and this, obviously, gives a meaningless answer.

The failure loads calculated using this formula are tabulated in Table 3.1. For Sample No. 6 a negative denominator was obtained. It can be seen, therefore, that at $\alpha = 30^o$ and K = 0,8 the theoretical strength, in this mode, is 375 kN; whereas for K = 0,64 the sample will not fail in this mode. Obviously, as the calculated strength becomes higher, other modes (e.g. branch cracks and spalling) tend to occur more often. This observation is born out by the fact that of the five samples with the largest strengths (i.e. Nos. 6, 64, 66, 70 and 1), only one shows no sign of branch cracks or axial tension cleavage.

For all "reasonable" values of α (i.e. $\alpha \geq 38^o$) the average experimental failure loads are all greater than the calculated values; so that if one was going to assume that the sample strength was made up of a peak intact material strength value plus that fraction of the joint strength developed at the same strain, one would have to conclude that all of the joint strength was mobilized.

TABLE 3.1

SAMPLE NO.	α (°)	k	CALCULATED (kN)	AV. EXPTL (kN)	REMARKS
1	38	0,71	39,6	40,9	MODE DOESN'T APPLY
6	30	0,64	DOESN'T FAIL	50,0	TOO STRONG, ∴ BRANCH CRACKS
62, 65, 68	50	0,8	13,0	17,0	MODE APPLIES
63, 67, 69	40	0,8	20,3	21,3	MODE APPLIES
64, 66, 70	30	0,8	375	44,6	MODE APPLIES (?)

3.2 Class 2 Calculations

The mode of failure assumed for these calculations is a shearing failure along the joints, a tension failure between, and at right angles to, the joints with a shearing failure occurring through the intact material on the extension of the joint if required. This mode allows the following resisting forces to be taken into account:

1. a shearing force provided by the joints,
2. a tensile force provided by the material between the joints, and
3. a shearing force provided by the material between the joints over an area of (L x the thickness of the sample).

For calculation purposes it should be noted that:

1. L cannot have a value less than zero, i.e. when the joints overlap there is is no negative component of strength due to the intact material, and
2. $L_{j\alpha}$ cannot have a value greater than that for which L = 0. (A mode using a greater value for $L_{j\alpha}$ could not be giving a minimum strength).

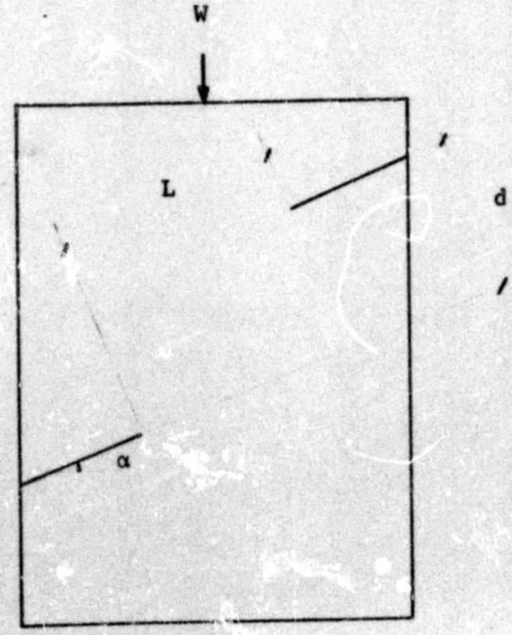

As before: DF = RF

$$W \sin\alpha = T.L\,(C_m + \sigma_n \tan\phi_m) + d.T.t_m + A_j\,(C_j + \sigma_n \tan\phi_j)$$

which gives

$$W = \frac{T\,(C_m.L + d.t_m + L_{j\alpha}.C_j)}{\sin\alpha - T.\cos^2\alpha\,(L.\tan\phi_m + L_{j\alpha}\tan\phi_j)/A}$$

For plaster of paris (t_m = 1,49 MPa, C_j = 0,0088 MPa, $\phi_j = 26^o$, C_m = 1,4 MPa and $\phi_m = 41^o$) and our samples (T = 51 mm, $\alpha = 39^o$ and A = 2 x 9 x $25,4^2$ mm^2) we get

$$W = \frac{51\,(1,4L + 1,49d + 0,0088\,L_{j\alpha})}{0,629 - 0,00602\,(0,38L + 0,213\,L_{j\alpha})}.$$

TABLE 3.2

Failure loads of Class 2 samples.

SAMPLE NOS.	d (mm)	L (mm)	CALCULATED (kN)	AV. EXPTL. (kN)
49, 24, 25, 26, 30, 31	51	0	20,4	16,8
10, 15, 16, 27, 28, 29	51	81	82,6	22,7
11, 17, 18, 19, 21, 22	51	158	391	37,2
33, 34, 35, 43	25	0	9,03	18,2
44, 45, 46, 47, 48	25	36	24,0	31,4
36, 37, 38, 49	25	74	48,9	32,2

The failure strengths calculated from this formula are tabulated in Table 3.2. In both cases (d = 51 mm and d = 25 mm) the calculated and average experimental strengths increase with increasing L. However, it can be seen that as the calculated strengths get larger, the experimental strengths fall far short of these calculated values (Figure 3.1.1). The reason for this is that as the calculated failure mode becomes stronger, other modes become more likely and, in fact, replace it. (For the configuration giving a calculated strength of 391 kN, 5 out of the 6 samples tested showed definite signs of branch cracks occurring).

From a comparison of the strengths, the conclusion must be drawn that, especially at higher strengths the calculated values do not fit the experimental strengths. This is, however, explained by the fact that other failure modes (e.g. branch cracks, axial clearage and spalling) are now preferred.

FIGURE 3.1.1

EXPERIMENTAL vs CALCULATED STRENGTHS

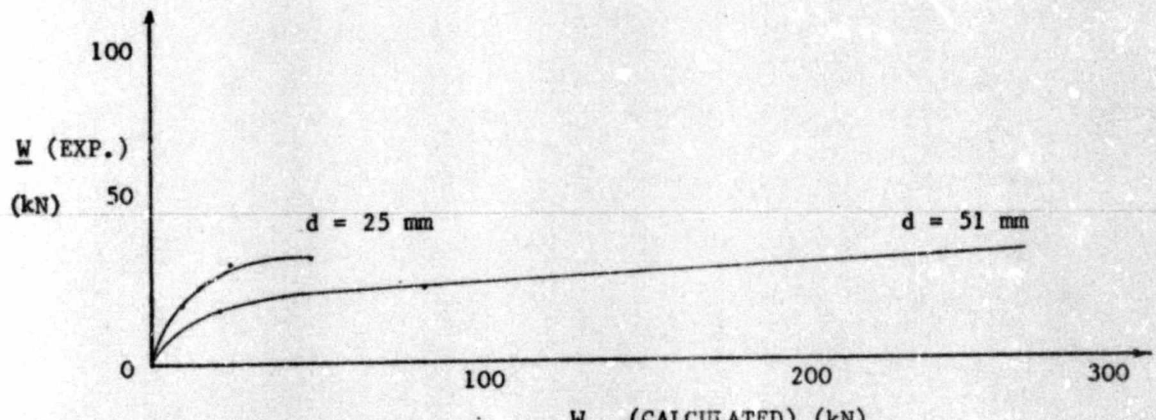

3.3 Class 3 Calculations

As already mentioned, Class 3 is a special case of Class 2, where the ψ-joint defines the position at which the fracture steps from one α-joint to the next. If one assumes that peak strength is reached before separation along the ψ-joint occurs, then the Class 2 failure strength formula applies (provided that the ψ-joint is assumed to contribute nothing to the failure strength).

From the formula we get

$$W = \frac{51\ (1{,}4L + 1{,}49d + 0{,}0088\ L_{j\alpha})}{0{,}636 - 0{,}00595\ (0{,}38L + 0{,}213\ L_{j\alpha})}\ \text{N} \quad (\alpha = 39\tfrac{1}{2}^{0})$$

$$= \frac{51\ (0 + 19{,}4 + 2{,}8)}{0{,}636 - 0{,}00595\ (0 + 67{,}9)}\ \text{N}$$

$$= \frac{51 \times 22{,}2}{0{,}636 - 0{,}404} = \frac{1132}{0{,}232} = 4\ 880\ \text{N}$$

In this case the actual failure mode was very close to the postulated failure mode, but the actual failure strength (less than 2,7 kN) does not compare very favourably with the calculated strength. If one assumes that the peak strength is reached after separation has occurred along the ψ-joint, and that the normal average stress in the α-direction on the β-plane is

$$\sigma_{n1} = \frac{W \cos \alpha}{A/\cos \alpha - \Sigma L_{j\psi p\alpha}},$$

then the contribution to the resisting force from joint shear is increased, and the failure load also increases. This can be shown algebraically as follows:

$$W \sin\alpha = T.L\,(C_m + \sigma_{ni} \tan\phi_m) + d.T.t_m + A_j\,(C_j + \sigma_{ni} \tan\phi_j)$$

which gives

$$W = \frac{T\,(L.C_m + d.t_m + L_{j\alpha}.C_j)}{\sin\alpha - \dfrac{T.L.\tan\phi_m.\cos\alpha}{A/\cos\alpha - T.\Sigma L_{j\psi p\alpha}} - \dfrac{A_j.\cos\alpha.\tan\phi_j}{A/\cos\alpha - T.\Sigma.L_{j\psi p\alpha}}}$$

$$= \frac{T\,(L.C_m + d.t_m + L_{j\alpha}.C_j)}{\sin - \dfrac{T\cos^2\alpha(L.\tan\phi_m + L_{j\alpha}.\tan\phi_j)}{A - T.\Sigma L_{j\psi p\alpha}.\cos\alpha}}$$

This formula gives a higher value of W than that obtained from the formula derived in 3.2 and thus compares even less favourably with the experimental value. Comparison with one measured value does, however, have its limitations.

A formula similar to that in the previous paragraph can be derived for the Class 4 configurations. However, as the experimental results are closer to the lower failure load values obtained when making the assumption that peak load is reached before separation; this assumption has been used for the Class 4 calculations.